Study of ZnO, SnO₂ and Compounds ZTO Structures Synthesized for Gas-Detection

Dr. Farhad M. Othman
Materials Engineering Department, University of Technology/Baghdad.
Email:fmok4@yahoo.com
Dr. Alaa A. Abdul-Hamead
Materials Engineering. Department, University of Technology/Baghdad.
Email:adr.alaa@yahoo.com
Alaa S. Taeeh
Materials Engineering Department, University of Technology/Baghdad.

ABSTRACT

Semiconductor-based metal oxide gas detector of five mixed Z:S from zinc chloride salt (0,25,50,75,100%) ratios with tin chloride salt, were fabricated on glass substrate by a spray pyrolysis technique with thickness were about (0.2 ± 0.05 μm) using water soluble as precursors at a substrate temperature 500 C°±5, 0.05 M ,and their gas sensing properties toward (CO_2 , NO_2 and SO_2 gas at different concentration (10,100,1000 ppm) in air were investigated at room temperature which related with the petroleum industry.

Furthermore structural and morphology properties was inspecting. Experimental results show that the mixing ratio affect the composition of formative oxides ($ZnO,Zn_2SnO_4,Zn_2SnO_4+ZnSnO_3,ZnSnO_3$, SnO_2) ratios mentioned in the above respectively, and related with the sensitivity of the tested oxidation gases.

Keyword: Zinc stannate, gas sensor, ternary metal oxides, spray pyrolyess, pollutant gases, XRD.

دراسة تراكيب SnO₂,ZnO و مركباتها ZTO المؤلفة على الكشف الغازي

الخلاصة:

في هذا البحث حضر كاشف شبه موصل اوكسيدي من خمس خلطاتZ:S من ملح كلوريد الزنك (100, 75 ,50, 25,0%) مع ملح كلوريد القصديرحضرت و بطريقة الرش الكيميائي الحراري و بسمك حوالي ($0.2 \pm$ 0.05 μm) على قواعد من الزجاج و باستخدام الماء كمذيب , و بدرجات حرارة ترسيب بلغت C° (5± 500) و بتراكيز M (0.05) ككاشف للغازات الملوثة مثل(CO_2 , NO_2 و SO_2) و بتركيز (10,100,1000 ppm) في الهواء و بدرجة حرارة الغرفة والمرتبطة مع الصناعة النفطية.

تم تشخيص التبلور و مورفولوجية سطح الأغشية المحضرة بواسطة قياسات حيود الأشعة السينية XRD و المجهر الالكتروني الماسح SEM ومجهرة القوة الذري AFMلها . بينت النتائج أن نسبة الخلط تؤثر على تبلور الأكاسيد المتكونة و المركبات الثلاثية المتكونة حيث كانت ($ZnO,Zn_2SnO_4,Zn_2SnO_4+ZnSnO_3,ZnSnO_3$, SnO_2) للنسب المذكورة في أعلاه على التوالي وترتبط مع حساسية الغازات المؤكسدة المفحوصة.

INTRODUCTION

T he development of high performance solid state chemical sensors is nowadays of outmost importance in many advanced technological fields[1]. Numerous researches have shown that a characteristic of solid-state gas sensors is the reversible interaction of the gas with the surface of a solid-state material. In addition to the conductivity change of gas-sensing material, the detection of this reaction can be performed by measuring the change of capacitance, work function, mass, optical characteristics or reaction energy released by the gas/solid interaction. Various materials, synthesized in the form of porous ceramic, and deposited in the form of thick or thin films, are used as active layers in such gas-sensing devices [2] . Zinc stannate or zinc tin oxide (ZTO) is a class of ternary oxides that are known for their stable properties under extreme conditions, higher electron mobility compared to its binary counterparts and other interesting properties. These materials is thus ideal for applications from, gas detector, solar cells photocatalysts, light-emitting diodes, field effect transistors and (heterojunction and homojunction) diodes. In 2000, K. Zakrzewska,[3] study mixed-oxide systems such as SnO$_2$-WO$_3$, TiO$_2$-WO$_3$ and SnO$_2$ - TiO$_2$ with the ultimate aim of the application in gas sensing devices and study dynamic changes in the electrical resistance (R) of SnO$_2$-WO$_3$ thin films for samples deposited at two different substrate temperatures, 100 and 300C° upon exposure it to hydrogen at 400C° and CH$_4$ at (350 , 700 C°). In 2006, S. M. Chou, L. G. Teoh, et. al., [4] study ZnO:Al thin film gas sensor for detection of ethanol vapor (400 ppm) at 250 C°.In 2007, M.Y. Faizah , A. Fakhru'l-Razi, et.al., [5] study gas sensor application of carbon nano tubes for (H$_2$, CO$_2$ and NH$_3$) gases at temperature higher than 200 C°.
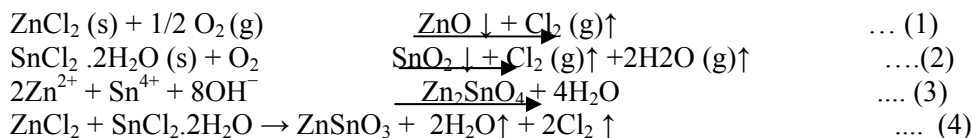
In 2008, L. Al-Mashat, H. D. Tran,et. al., [6] study conductometric hydrogen gas sensor based on polypyrrole (PPy) nanofibers at temperature below (100 C°).The goal of this work is to fabricating different semiconductor-based metal oxide gas detector of five mixed film by spray pyrolysis technique , and study some of their structural properties and sensitivity to some pollutant gases .

Experimental Work

The work includes the following steps;

The First Step:

• Preparation of an aqueous solution of zinc chloride (ZnCl$_2$ and SnCl$_2$.2H$_2$O) with purities 99.9%, at (0,25,50,75,100)% ratios .

• The concentration was (0.05 M), the acidity was maintained to be ≈5.5 pH during spraying .The spraying apparatus was manufactured locally in the university laboratories. In this technique, the prepared aqueous solutions were atomized by a special nozzle glass sprayer at heated collector glass fixed at thermostatic controlled hot plate heater.

• Air was used as a carrier gas to atomize the spray solution with the help of an air compressor with pressure (7 Bar) air flow rate (8 cm^3/sec) at room temperature.

• The glass substrate(0.1 cm thickness) temperature was maintained at 500 °C during spraying , coating thickness was(0.2) μm by tested by optical microscopy.

• Atomization rate was (1 nm/s) with (2.5 ml/min) of feeding rate. The distance between the collector and spray nozzle was kept at (30 ±1 cm) the volume of spray solution was 50 ml , number of spraying (100) ,time between two spraying (10 sec).

• The spray of the aqueous solution yields the following chemical reaction [7,8,9]:

•

$$ZnCl_2 \text{ (s)} + 1/2\ O_2 \text{ (g)} \longrightarrow ZnO \downarrow + Cl_2 \text{ (g)} \uparrow \qquad \qquad \dots (1)$$
$$SnCl_2 .2H_2O \text{ (s)} + O_2 \longrightarrow SnO_2 \downarrow + Cl_2 \text{ (g)} \uparrow + 2H2O \text{ (g)} \uparrow \qquad \dots (2)$$
$$2Zn^{2+} + Sn^{4+} + 8OH^- \longrightarrow Zn_2SnO_4 + 4H_2O \qquad \qquad \dots (3)$$
$$ZnCl_2 + SnCl_2.2H_2O \rightarrow ZnSnO_3 + 2H_2O \uparrow + 2Cl_2 \uparrow \qquad \qquad \dots (4)$$

The Second Step:
   Spraying the solution on the substrate at temperature(500 ±5°C)[10,11].

The Third Step: Annealing samples, by using furnace(type Nabertherm) at temperature 500˚C for (60 min) and cooling inside furnace.

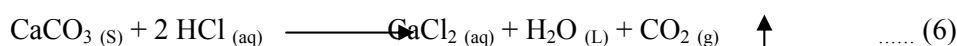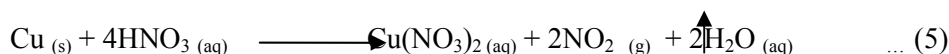**The Forth Step :**
Inspection which include:
1- X-ray diffraction by diffractometer type with radiation CuKα (λ = 1.5406 Å). This inspection was carried out in Advanced Materials Research Center at the Technology and Science Ministry, with continuous scanning.
2-   Scanning Electron Microscopy (SEM):The SEM study has been carried out by Electron Gun Tungsten heated filament, Resolution 3 nm at 30kV, Accelerating voltage 200 V to 30kV, chamber internal size : 160 mm (Japan) ,with Au coating for(20 sec).The setting in Nano Center at University of Technology.
3- Atomic Force Microscopy (AFM) :It was taken with a digital instruments, typical data has been taken from AFM height images include root mean square (RMS) and roughness .Made in USA, model AA3000 220V.
4- gas-sensing :The gas-sensing experiments were carried out by introducing the thus prepared devices into a home-made test cell, which was consist of a cylinder with cover to restrict prepared gas as in figure (1) .
The gas was obtained from reaction solution to rising predicted gases. pollutant gases that prepared CO_2 ,NO_2 and SO_2 gases as will be explained in the following produce from reactions equation: [7,10]

$$Cu_{(s)} + 4HNO_3\ _{(aq)} \longrightarrow Cu(NO_3)_2\ _{(aq)} + 2NO_2\ _{(g)} + 2H_2O_{(aq)} \qquad \dots (5)$$

$$CaCO_3\ _{(S)} + 2\ HCl_{(aq)} \longrightarrow CaCl_2\ _{(aq)} + H_2O_{(L)} + CO_2\ _{(g)} \uparrow \qquad \dots (6)$$

$$Cu_{(s)} + 2H_2SO_{4(aq)} \longrightarrow CuSO_4\ _{(aq)} + SO_2\ _{(g)} + 2H_2O_{(aq)} \qquad \dots (7)$$

   The gases -sensing properties were determined at different temperature by measurement of the electrical conductivity of the samples which exposed to various concentration of the gases (10, 100,1000) ppm_v[12,13]. The sensor response was defined using the following equation[14,15]:

$$\text{Sensor response (\%)} = [(Ra - Rg)/Ra] \times 100\% \qquad \qquad \dots (8)$$
Where
 Ra and Rg are the electric resistance in air and test gas, respectively.

Results and Discussion
1-   X-ray results, the result of X-ray diffraction which represent all mixing ratio for precipitation thin films on glass substrates are shows in Fig.(2) the XRD patterns

result shows match with standard value in (JCPDS card No. 36-1451). ZnO have wurtzite type polycrystalline thin film with a hexagonal system revealing that the highly dominant to c-axis oriented the film was grown, no characteristic peaks for any other impurities were observed, suggesting   sample have high purity. The *c*-axis orientation in ZnO films can be understood by the "survival of the fastest" model, in where nuclei having the fastest growth rate can survive, i.e., *c*-axis orientation is achieved [16,17].

In Fig.(3) it can be seen that the mixing (ZTO) of components di-zinc stannate Zn_2SnO_4 and scant traces of zinc stannate $ZnSnO_3$. according to standard cards (JCPDS card No.24-1470 and No.28-1486) respectively. The Zn_2SnO_4 have high appearance comparing with $ZnSnO_3$ because of large accoutrement of Zn ion in mixing [18]. All of the diffraction peaks well match the standard diffraction pattern of cubic spinal structure for Zn_2SnO_4 , while $ZnSnO_3$ has a perovskite face-centered structure, coinciding with [19,20,21]. A different mixing ratio of (ZTO) is shown in Fig. (4) of components zinc stannate ($ZnSnO_3$) and di-zinic stannate (Zn_2SnO_4) return to show, by more than one peak the mixture homogenized showing deposition efficiency as well as the proper role of annealing in the formation of both two compounds according to stander cards. Another mixing ratio ($Z_{0.25}:S_{0.75}$) is shown in fig.(5) , $ZnSnO_3$ appears and it has high appearance comparing with Zn_2SnO_4 because of large amount of supplying of Sn ions in mixing. The highest peaks for the compound $ZnSnO_3$, and for Zn_2SnO_4 more than one weak peaks was observed as shown in table (1). Finally in Fig. (6), which is represent mixing ratio of salts (0% zinc oxide and 100% of the tin oxide),SnO_2 pattern of film was much with standard card (JCPDS No.41-1445) have tetragonal rutile structure, no characteristic peaks for any other oxides or impurities were observed, suggesting   sample have high purity oxide. Table (1) shows results Data of XRD $Z_1:S_0$ and $Z_0:S_1$ and table (2)   Results XRD Data for other Z:S mixing ratios.

2-   SEM :Micrographe

Fig.(7) shows ZnO (2D-images), the film deposited with zinc is formed a hexagonal, this is consistent with XRD analysis. The latter corresponds to the diffraction plane (002) in the hexagonal wurtzite structure of ZnO. The appearance of the preferential diffraction peak, assigned to the plane (002), indicates that the film growth is achieved along the axis c of the hexagonal structure normal to the substrate surface as show in Fig (7), this is good harmony with the SEM observation for (N. Lehraki *et al*) [21]. The ortho stable form of zinc stannate (Zn_2SnO_4) have tri-symmetric face-center cubic spinel structure, SEM (2-D) images for growth Zn_2SnO_4 show the morphology of microcubes at different magnifications Fig.(8), this is good concordance with the SEM observation for (S. Baruah and J. Dutta) [8]. SEM (2-D) images for growth Zn_2SnO_4 and $ZnSnO_3$ microcubes at different magnifications are shown in Fig.(9). Zinc stannate ($ZnSnO_3$) has structure perovskite, according to results XRD which shows almost all the particles are spherical in shape leaving some space between them as shown in Fig. (10), this is good matching with the SEM observation for (R. Singh *et. al.*) [22].   SEM (2D-images) obtained for $Z_0:S_1$ represented by SnO_2 pure film for sensor application are shown in Fig.(11), summarizes the scanning electron microscopy (SEM) analysis of the SnO_2 deposit have a large area from the surface of the deposit is homogeneous [23].

3-   AFM result

AFM is powerful technique to investigate the surface morphology at nano to microscale. The surfaces of the films are shown in Figs.(12,13,14,15,16) for mixing (1, 0.75, 0.5, 0.25, 0)% of Z respectively. Irregularities in the film surface (top view) from

the spray technique, which benefited tremendously for the gas sensing properties [24]. The surfaces morphology of the ZnO films as observed from the (3-D) AFM micrograph figs. (12,13,14,15,16) confirms that the grains were uniformly distributed within the scanning area (2014 X 2014) nm. This surface characteristic is important for applications gas sensors [26].The roughness was found 19.62 nm and average diameter 76.06 nm, For Zn_2SnO_4 .In fig.(13) the roughness was 18.14 nm and average diameter 91.33 nm, and in fig.(14) the roughness was found 6.72 nm and average diameter 109.99 nm, fig.15 shows $ZnSnO_3$ surface with roughness was found 4.80 nm and average diameter 81.20 nm .Fig.16 shows surface morphology of SnO_2 with roughness 22.94 nm and average diameter 68.31 nm.

4- Gas Sensor Results

 For the investigation of the oxidation gases sensing properties of the Z:S oxide films , the optimum operation gas temperature should be fixed at the first. Fig. (17), shows an increasing the response of sensor by increased SO_2 gas concentration on the one hand and increased in response with variation of   Z:S oxide ratio ,which resulted in change oxides consisting as it was seen in XRD results, the difference broad here since low concentrations of the gas between the pure oxides and mixtures are obey to the same relationship for oxidation gases[26].

$$O_2 \,(g) + e^- \rightarrow O_2^- \,(ads) \qquad\qquad\qquad \text{..... (9)}$$

   It can be observed that sensors based on pure oxide ZnO and SnO_2 show relatively low response at the same operating temperature in the range from (10 - 1000)ppm,with the maximum response of (88. 39 %) and(90.87 %) for ZnO and SnO_2 at 1000 ppm , respectively. In contrast, sensor with mixed oxides (Zn_2SnO_4 , $ZnSnO_3$) exhibits an increase of response to reach the maximum value of 100% at the 1000 pm concentration of SO_2 gas for them . Fig.(18) shows the response time as a function of gas concentration   ,it can be seen that the time diminish by increased gas concentration[27-28].

In the presence of NO_2 in air the sample's sensitivity is shown in Fig.(19) acceptor gas adsorption[29] :

$$NO_{2(gas)} + \overline{e} \leftrightarrow N\overline{O}_{2(ads)} \qquad\qquad\qquad \text{…(10)}$$

The same equation (9)
where :
 NO_2 :molecule in the gas phase
 e^- :an electron from the conduction band of the semiconductor
 $NO^-_{2(ads)}$:adsorbed form of NO_2 on the semiconductor surface.

 This indicates the role of the electronic factor in the sensor sensitivity. After the adsorption on the surface the NO_2 molecule acts as an electronic trap, profoundly depleting the electron density in the conduction band and leading to a significant decrease of the crystalline material conductance , and this indicates the role of the electronic factor in the sensor sensitivity[30].   So, an increase of concentration of electrons, which have enough energy to overcome the electric barrier resulting from the negative charging of the surface, favors reaction that leads to an increase of the sensor signal. It can be observed that sensors based on pure oxide ZnO and SnO_2 show relatively low response at the same operating temperature in the range from (10 - 1000)ppm , with the maximum response of (80. 0 %) and (84.44 %) for ZnO and SnO_2 at 1000 ppm , respectively. In contrast, sensor with mixed oxides (Zn_2SnO_4 , $ZnSnO_3$)

exhibits an increase of response to reach the maximum value of (90.97%) at the 1000 pm concentration of NO$_2$ gas for them .

Fig.(20) shows the response time as a function of gas concentration, it can be seen that the time diminish by increased gas concentration . And it is higher for pure oxide and fewer for mixed oxides.
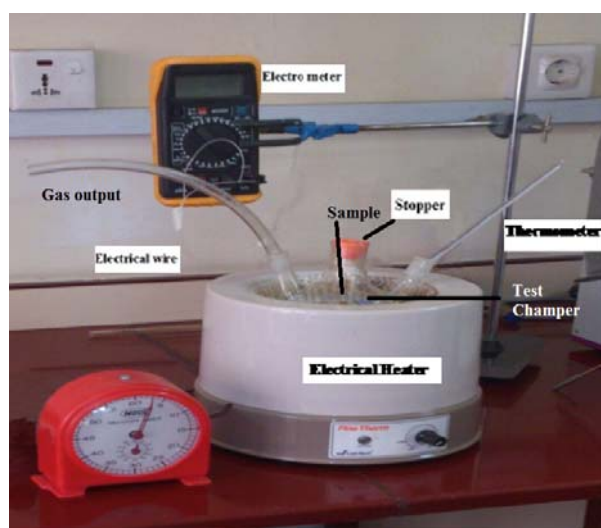
Fig.(21) shows an increasing the response of sensor by increased CO$_2$ gas concentration on the one hand and an increased in response with variation of Z:S Oxide ratio. As shown in the figure, when O$_2$ molecules are adsorbed on the surface of metal oxides, they would extract electrons from the conduction band Ec and trap the electrons at the surface in the form of ions, differences in the nature of the interaction with different gas CO$_2$ from NO$_2$ and SO$_2$gas on the one hand the length of the bond, and enthalpy .Also the influence of the crystallite which found in sensitivity[29,30]. This will lead a band bending and an electron depleted region. The electron-depleted region is so called space-charge layer, of which thickness is the length of band bending region. Reaction of these oxygen species with reducing gases or a competitive adsorption and replacement of the adsorbed oxygen by other molecules decreases and can reverse the band bending, resulting in an increased conductivity. O− is believed to be dominant at the operating temperature which is the work temperature for most metal oxide gas sensors [21,31] .It can be observed that sensors based on pure oxide ZnO and SnO$_2$ show relatively low response at the same operating temperature in the range from (10 - 1000)ppm , with the maximum response of (78. 48 %) and (80.54 %) for ZnO and SnO$_2$ at 1000 ppm , respectively. In contrast, sensor with mixed oxides (Zn$_2$SnO$_4$, ZnSnO$_3$) exhibits an increase of response to reach the maximum value of (91.62%) at the 1000 pm concentration of CO$_2$ gas for them . Fig.(22) shows the response time as a function of gas concentration ,it can be seen that the time diminish by increased gas concentration. And it is higher for pure oxide and fewer for mixed oxides. Less response time was (40-17 sec) for (10-1000 ppm) , starting response times for the pure oxide films(ZnO,SnO$_2$) were about (9 sec) and for mixed oxide less than (4 sec).

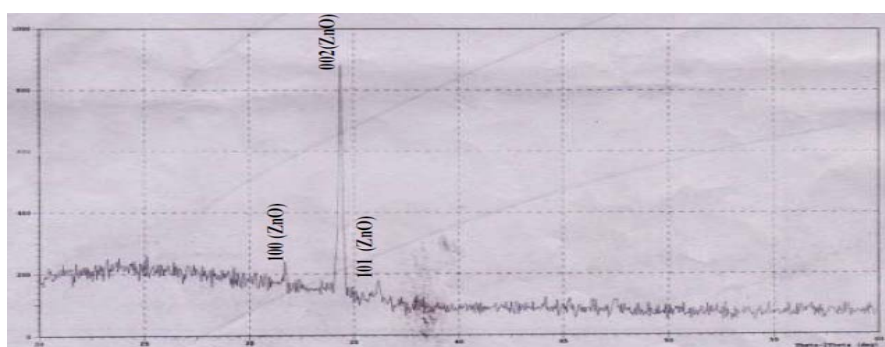**Table (1)   Results data of XRD Z$_1$:S$_0$ and Z$_0$:S$_1$**

Mix	Comp.	2θ$_{ST}$	2θ$_M$	I$_{ST}$%	I$_M$%	hkl
Z$_1$:S$_0$	ZnO	31.770	31.762	57	13	100
		34.422	34.409	44	100	002
		36.253	36.248	100	9	101
Z$_0$:S$_1$	SnO$_2$	26.611	26.5586	100	100	110
		33.893	33.8393	75	54	101
		37.950	37.8356	21	17	200
		51.781	51.6776	57	38	211
		54.759	54.6263	14	11	220

Table (2)   Results XRD data of other Z:S mixing ratio

Comp.	$2\theta_{ST}$	$I_{ST}\%$	hkl	$Z_{0.75}:S_{0.25}$		$Z_{0.5}:S_{0.5}$		$Z_{0.25}:S_{0.75}$	
				$2\theta_M$	$I_M\%$	$2\theta_M$	$I_M\%$	$2\theta_M$	$I_M\%$
Zn$_2$SnO$_4$	29.141	19	220	29.1028	20	29.1028	20	29.1445	20
	34.291	100	311	34.1384	100	34.1384	100	34.2381	20
	35.907	20	222	35.6376	20	35.6376	20	35.2377	17
	41.685	25	400	41.2080	22	41.2080	22	41.5911	17
	55.116	30	511	--	--	55.1061	30	--	--
ZnSnO$_3$	26.507	100	012	26.3902	22	26.4140	39	26.4357	100
	33.797	50	110	--	--	33.5053	61	33.6520	44
	37.768	20	015	--	--	37.7356	39	37.6106	31
	51.596	45	116	--	--	51.5212	30	--	--
	57.559	3	018	--	--	57.5252	13	--	--

Figure(1) Gas detection measurement system

Figure(2) XRD result spectra of Z$_1$:S$_0$/glass

Figure(3) XRD result spectra of Z₀.₇₅:S₀.₂₅/glass

Figure(4)   XRD result spectra of Z₀.₅:S₀.₅/glass

Figure(5) XRD Spectra of Z₀.₂₅:S₀.₇₅/glass

Figure(6)   XRD result spectra of Z₀:S₁/glass

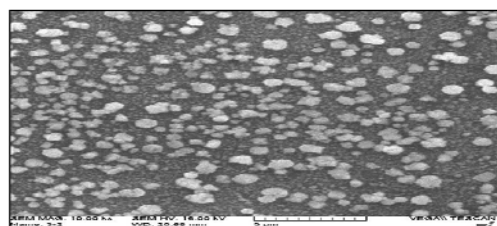**Figure(7)(SEM) micrographs image for Z$_1$:S$_0$**

Figure.(12) 3-D AFM image of the Z$_1$: S$_0$
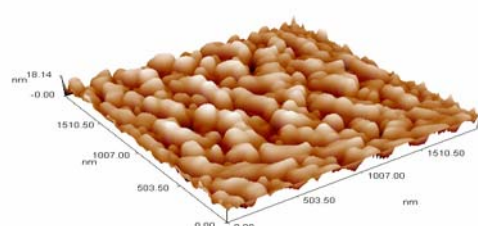

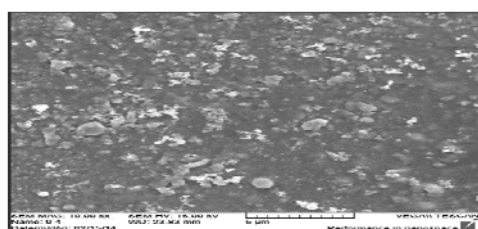**Figure(8)(SEM)micrographs image for Z$_{0.75}$:S$_{0.25}$**

Figure.(13)3-D AFM image oftheZ$_{0.75}$: S$_{0.25}$

Figure(9)SEM micrographs image for Z$_{0.5}$:S$_{0.5}$

Figure.(14) 3-D AFM image of the Z$_{0.5}$: S$_{0.5}$
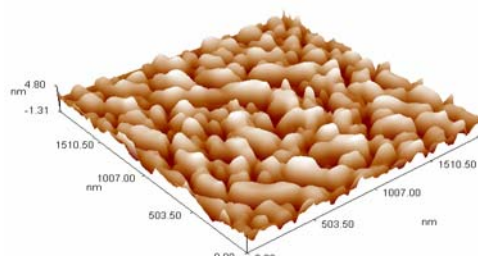

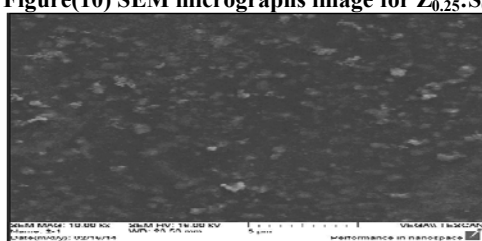**Figure(10) SEM micrographs image for Z$_{0.25}$:S$_{0.75}$**

Figure.(15) 3-D AFM image of the Z$_{0.25}$: S$_{0.75}$
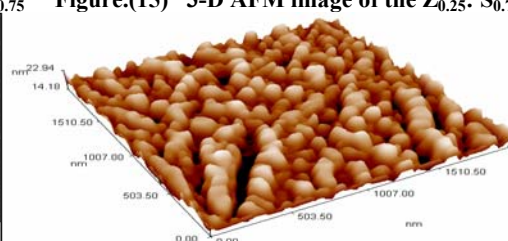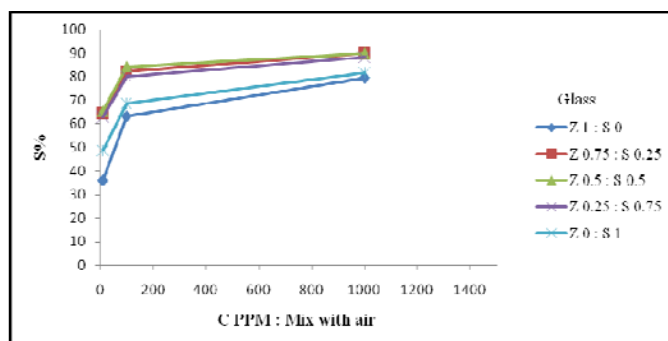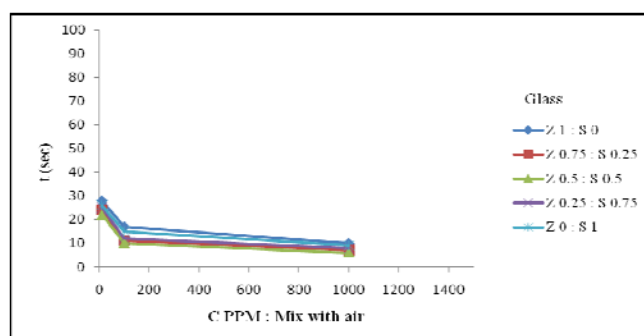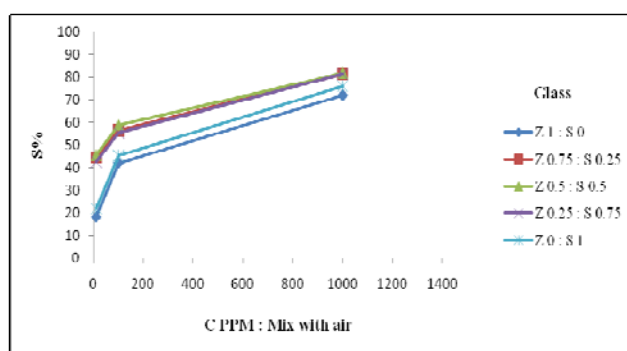

Figure(11)SEM micrographs image for Z$_0$:S$_1$

Figure.(16) 3-D AFM image of the Z$_0$: S$_1$

Figure(17) Gas sensitivity for SO₂

Figure(18)   Response time for SO₂

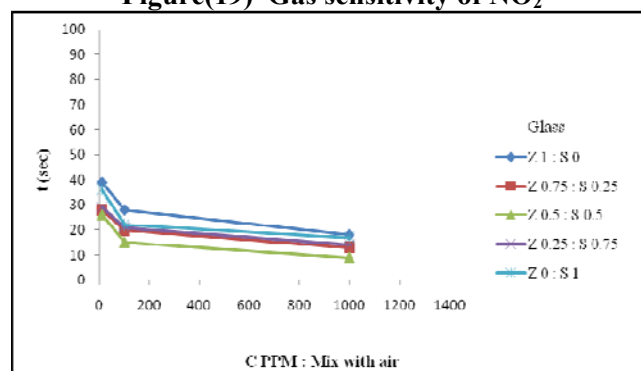**Figure(19) Gas sensitivity of NO₂**

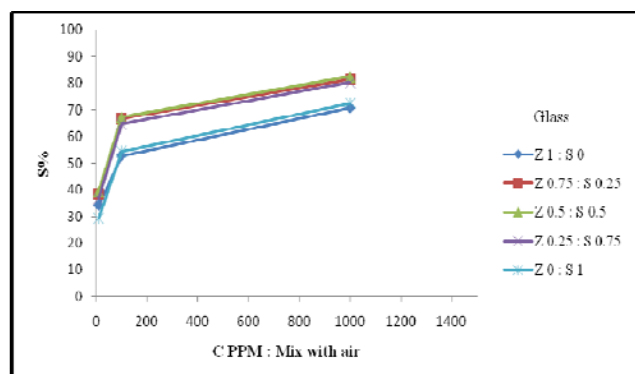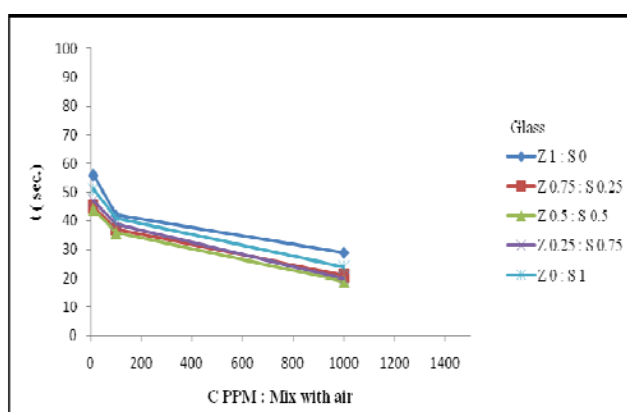**Figure (20)   Response time for NO₂**

Figure (21)   Gas sensitivity for CO$_2$

Figure(22) Response time for CO$_2$ gas

CONCLUSIONS

1-   Preparing gas sensor with several oxides form of (ZnO, Zn$_2$SnO$_4$, ZnSnO$_3$, SnO$_2$) on glass substrates to detect different gases.

2-   Mixing ratios chloride salts generate oxide compounds (triple and binary) with different responses for different testing gases.

3-   Homogenous surface of thin films and crystalline structures; hexagonal, tetragonal and cubic for oxides ZnO, SnO$_2$, ZnSnO$_3$ and Zn$_2$SnO$_4$ respectively. Mixing oxides (Zn$_2$SnO$_4$+ ZnSnO$_3$) showed the highest response rate for all testing gases at the best possible time.

REFERENCES

[1] G. Neri, "Metal oxide nanostructures for solid state gas sensors: A Recent patent survey", Recent patents on Materials Science, Vol. 4, PP. 146-158, (2011).

[2] G. Korotcenkov, "Metal oxides for solid-state gas sensors: What determines our choice?", Materials Science and Engineering B, Vol. 139, PP. 1–23, (2007).

[3] K. Zakrzewska, "Mixed oxides as gas sensors", Thin solid films, Vol. 391, PP. 229-238, (2001).

[4] S. M. Chou, L. G. Teoh, W. H. Lai, Y. H. Su and M. H. Hon, "ZnO:Al Thin film gas sensor for detection of ethanol vapor", Sensors, Vol. 6, PP. 1420-1427, (2006).

[5] M.Y. Faizah, A. Fakhru'l-Razi, R. M. Sidek and A. G. L. Abdullah, "Gas sensor application of carbon nanotubes", International Journal of Engineering and Technology, Vol. 4, No. 1, pp. 106-113, (2007).

[6] L. Al-Mashat, H. D. Tran and W. Wlodarski,, "Conductometric hydrogen gas sensor based on polypyrrole nanofibers", IEEE Sensors Journal , Vol. 8, No.4,(2008).

[7] Cleveland, Ohio, CRC Handbook of Chemistry and Physics 1978.

[8] S. Baruah, J. Dutta, "Zinc stannate nanostructures: Hydrothermal synthesis", Sci. Technol. Adv. Mater., Vol. 12, PP. 18, (2011).

[9] L.A. Patil, I.G. Pathan, "Spray pyrolyzed ZnSnO$_3$ nanostructured thin films for hydrogen sensing", Procedia Materials Science, Vol. 6, PP. 1557 – 1565, (2014).

[10] P. Patnaik, Handbook of Inorganic Chemicals, McGraw-Hill, (2003).

[11] A. H.Ataiwi &A.A. Abdul-Hamead, Study some of the structure properties of ZrO$_2$ ceramic coats prepared by spray pyrolysis method, Eng. & Tech. Journal, Vol.27, No.16, 2009.

[12] M. Kojim, "The Role of liquefied petroleum gas in reducing energy poverty", Extrctive industrial for development series, Vol. 25, (2011).

[13] C. Woong , S.Park& J. Lee, Punched ZnO nanobelt networks for highly sensitive gas sensors, Sensors and Actuators B: Chemical J., Sensors and Actuators, B174 ,PP.495– 499,(2012).

[14] S. Lee, S. Kim , B. Hwang , S. Jung,D. Ragupathy ," Improvement of H$_2$S Sensing Properties of SnO$_2$-Based Thick Film Gas Sensors Promoted with MoO$_3$ and NiO",Sensors,Vol. 13, PP.3889-3901,(2013).

[15] C.M. Mahajan, "An influence of deposition temperature on structural, optical and electrical properties of sprayed ZnO thin films of identical thickness", Current applied physics, Vol.13, Issue 9, PP. 2109–2116, (2013).

[16] A.MISIUK, Reflection X-ray Topography of ZnO Thin Films on Non-Orienting Substrates, Thin Solid Films, 76 (1981)83.

[17] K. Jeyadheepan, C. Sanjeeviraja, "Preparation and crystal structures of some A^{IV}B$_2$^{II}O$_4$ compounds: Powder X-Ray diffraction and rietveld analysis", Journal of chemistry, ID 245918, (2014).

[18] A. Salehi, M. Gholizade, "Gas-sensing properties of indium-doped SnO$_2$ thin films with variation in indium concentration", Sensor and actuators B, Vol.89, pp. 173-179, (2003).

[19] M. Miyauchi, Z. Liu, Z. Zhao, S. Anandan and K. Hara, "Single crystalline zinc stannate nanoparticles for efficient photo-electrochemical devices", Chemical communications , Vol. 46, PP. 1529-153, (2010).

[20] S. V. Ryabtsev, E. P. Domashevskaya and E. P. Domashevskaya, "Study of ZnO, SnO$_2$ and ZnO/SnO$_2$ nanostructures synthesized by the gas-transport", Condensed matter and interphase boundaries, Vol. 12, No. 1, PP. 17-21, (2010).

[21] N. Lehraki, M.S. Aida, S. Abed, N. Attaf, A. Attaf and M. Poulain, "ZnO thin films deposition by spray pyrolysis: Influence of precursor solution properties", Current applied physics,Vol.12, (2012).

[22] R. Singh, A. K. Yadav and C. Gautam, "Synthesis and humidity sensing investigations of nanostructured ZnSnO$_3$ ", Journal of sensor technology, Vol. 1, PP. 116-124, (2011).

[23] A. Salehi, M. Gholizade, "Gas-sensing properties of indium doped SnO$_2$ thin films with variation in indium concentration", Sensor and actuatore B, Vol. 89, PP. 173-179, (2003).

[24] F.A. Chyad,A.F. Hamood,L.S. Faiq, Effect of thermally sprayed ceramic coating on properties of low alloy steel,Eng. &Tech.Journal, Vol. 32,Part (A), No.10, 2014.

[25] Y.C. Ji, H.X. Zhang, X.H. Zhang and Z.Q. Li ,"Structures, optical properties, and electrical transport processes of SnO_2 films with oxygen deficiencies", Cond-mat.mtrl-sci, Vol. 1, (2013).

[26] G.F. Fine, L. M. Cavanagh, et. al., "Metal oxide semi-conductor gas sensors in environmental monitoring", Sensors, Vol. 10, PP.5469-5502, (2010).

[27] Q. G. Hial, "Improvement of ZnO and SnO_2 hydrogen gas sensors", PhD Thesis University of Baghdad, Iraq, (2011).

[28] F.N. Jiménez-García, C.L. Londoño-Calderón, D.G. E. Arbeláez, A. Real and M. E. Rodríguez-García,, "Influence of substrate in structural, morphological, and optical properties of ZnO films grown by silar method", Journal of physics and chemistry of solids, Vol. 68, (2007).

[29] T. Akamatsu, T. Itoh, N. Izu and W. Shin, "NO and NO_2 sensing properties of WO_3 and Co_3O_4 based gas sensors", Sensors, Vol.13, PP. 12467-12481, (2013).

[30] X. Xue, Y. Nie, B. He, L. Xing, Y. Zhang and Z.Wang, "Surface free-carrier screening effect on the output of a ZnO nanowire nanogenerator and its potential as a self-powered active gas sensor", Nanotechnology, Vol. 24, PP.1-6, (2013).

[31] F. Fine, L. Cavanagh, A. Afonja and R. Binions," Metal oxide semi-conductor gas sensors in environmental monitoring", Sensors, Vol. 10, PP. 5469-5502, (2010).